Two-Photon Spectroscopy of *all-trans*-Retinal. Nature of the Low-Lying Singlet States[1]

Robert R. Birge,*[2a] James A. Bennett,[2a] Lynn M. Hubbard,[2a] Howard L. Fang,[2b] Brian M. Pierce,[2a] David S. Kliger,[2c] and George E. Leroi[2b]

Contribution from the Department of Chemistry, University of California, Riverside, California 92521, Department of Chemistry, Michigan State University, East Lansing, Michigan 48824, and the Division of Natural Sciences, University of California, Santa Cruz, California 95060. *Received April 24, 1981*

Abstract: The two-photon excitation spectrum of *all-trans*-retinal in EPA at 77 K is obtained over the wavelength region from 375 to 470 nm ($\lambda_{ex}/2$) using linearly polarized light. The two-photon spectrum is unstructured and is inhomogeneously broadened to the same degree observed for the one-photon absorption spectrum of *all-trans*-retinal. The two-photon excitation maximum is observed at ~428 nm ($\lambda_{ex}/2$) which is red shifted ~2400 cm^{-1} from the one-photon absorption maximum at ~388 nm. We assign the two-photon excitation spectrum to the "$^1A_g{}^{*-}$" state, although a least-squares fit of the spectrum to two log-normal curves indicates that the "$^1B_u{}^{*+}$" state also contributes roughly 15% of the band profile. We conclude that the two-photon absorptivity of the "$^1A_g{}^{*-}$" ← S_0 transition is at least five times larger than that observed for the "$^1B_u{}^{*+}$" ← S_0 transition (the least-squares fit calculates 6.9 ± 1.0). A complementary analysis of the one-photon absorption spectrum indicates that the one-photon oscillator strength of the "$^1B_u{}^{*+}$" ← S_0 transition is at least nine times larger than that observed for the "$^1A_g{}^{*-}$" ← S_0 transition. The "$^1A_g{}^{*-}$" state is therefore the lowest lying $\pi\pi^*$ state in *all-trans*-retinal and its absorptivity maximum is 2400 ± 300 cm^{-1} below the absorption maximum of the "$^1B_u{}^{*+}$" state in EPA (77 K). An approximate solvent effect calculation predicts a free chromophore "$^1B_u{}^{*+}$"–"$^1A_g{}^{*-}$" energy splitting of 4800 ± 900 cm^{-1}. INDO–PSDCI molecular orbital theory predicts that the "$^1A_g{}^{*-}$" and "$^1B_u{}^{*+}$" states in *all-trans*-retinal are "mixed" by a combination of conformational distortion and polarity effects and that these two perturbations are of approximately equal importance. The $n\pi^*$ state contributes a negligible fraction to the one-photon and two-photon band profiles. Although the "$^1A_g{}^{*-}$" $\pi\pi^*$ state is probably the lowest lying singlet state of *all-trans*-retinal in EPA (77 K), INDO–PSDCI calculations predict that the $n\pi^*$ state is the lowest lying singlet in nonpolar solvents.

I. Introduction

The level ordering of the low-lying excited singlet states of the visual chromophores has been the subject of extensive spectroscopic study and continuing controversy (see ref 3 for a recent review). The controversy is characterized by numerous conflicting assignments in the literature and is due in part to the inherent difficulty of spectroscopically assigning the excited states of molecules, like the visual chromophores, which are subject to severe inhomogeneous broadening in their electronic spectra. The excited singlet-state manifold of *all-trans*-retinal (Figure 1) provides a particularly challenging system to study because there are three low-lying states ["$^1B_u{}^{*+}$" ($\pi\pi^*$), "$^1A_g{}^{*-}$" ($\pi\pi^*$), and $^1n\pi^*$] that are very close in energy.[3,4] Furthermore, the relative level ordering appears to be solvent dependent.[5]

The location of the low-lying "forbidden" $^1A_g{}^{*-}$-like $\pi\pi^*$ state in the visual chromophores is believed to be of importance in defining the photochemical properties of these molecules.[3,6,7] Recent calculations indicate that the interaction of this state with a lowest lying "$^1B_u{}^{*+}$" state may be directly responsible for producing a barrierless excited-state potential energy surface for cis–trans isomerization of the chromophore in rhodopsin.[7] The extremely rapid formation of bathorhodopsin may therefore be a consequence of the photochemical lability of the "$^1A_g{}^{*-}$" state.[7]

The pioneering spectroscopic investigations of Hudson, Kohler, Christensen, and co-workers indicate that the forbidden $^1A_g{}^{*-}$ state is the lowest lying excited singlet in long-chain linear polyenes.[8–11] It is not possible, however, to generalize this level ordering to the visual chromophores because this covalent state is predicted to be highly sensitive to conformation and polarity.[3,6]

Two-photon spectroscopy has proven to be one of the most versatile methods of studying forbidden $^1A_g{}^{*-}$ and $^1A_g{}^{*-}$-like states.[11–18] This technique has verified the lowest energy position of this excited state in the linear polyenes diphenylbutadiene,[12,13] diphenylhexatriene,[14] diphenyloctatetraene,[15] and octatetraene[11] and in the visual chromophores *all-trans*-retinol[16] and *all-trans*-retinal.[17] Two-photon spectroscopy is particularly useful for studying the visual chromophores[16–18] because inhomogeneous broadening prevents the use of the high-resolution, low-temperature matrix techniques that have successfully been used to study the $^1A_g{}^{*-}$ state in the linear polyenes.[8,9]

Our preliminary two-photon excitation spectrum of *all-trans*-retinal covered a relatively small wavelength range from 410 to

(1) Abstracted in part from the Ph.D. theses of James A. Bennett, University of California—Riverside, 1980 (two-photon spectroscopy), and Lynn M. Hubbard, University of California—Riverside, 1980 (molecular orbital calculations).

(2) (a) University of California—Riverside. (b) Michigan State University. (c) University of California—Santa Cruz.

(3) Birge, R. R. *Annu. Rev. Biophys. Bioeng.* **1981**, *10*, 315–54.

(4) Symmetry classifications given in quotation marks are approximate and are derived by correlating the properties of a given electronic state with those of the analogous state in a linear polyene of C_{2h} symmetry. In other words, "$^1A_g{}^{*-}$" should be interpreted as $^1A_g{}^{*-}$-like.

(5) Takemura, T.; Das, P. K.; Hug, G.; Becker, R. S. *J. Am. Chem. Soc.* **1978**, *100*, 2626.

(6) Birge, R. R.; Schulten, K.; Karplus, M. *Chem. Phys. Lett.* **1975**, *31*, 451.

(7) Birge, R. R.; Hubbard, L. M. *J. Am. Chem. Soc.* **1980**, *102*, 2195; *Biophys. J.* **1981**, *34*, 517.

(8) Hudson, B. S.; Kohler, B. E. *J. Chem. Phys.* **1973**, *59*, 4984; *Annu. Rev. Phys. Chem.* **1975**, *25*, 437.

(9) Christensen, R. L.; Kohler, B. E. *Photochem. Photobiol.* **1973**, *18*, 293; *J. Phys. Chem.* **1976**, *80*, 2197.

(10) D'Amico, K. L.; Manos, C.; Christensen, R. L. *J. Am. Chem. Soc.* **1980**, *102*, 1777.

(11) Granville, M. F.; Holtom, G. R.; Kohler, B. E.; Christensen, R. L.; D'Amico, K. L. *J. Chem. Phys.* **1979**, *70*, 593.

(12) Bennett, J. A.; Birge, R. R. *J. Chem. Phys.* **1980**, *73*, 4234.

(13) Swofford, R. L.; McClain, W. M. *J. Chem. Phys.* **1973**, *59*, 5740.

(14) Fang, H. L.; Thrash, R. J.; Leroi, G. E. *Chem. Phys. Lett.* **1978**, *57*, 59.

(15) Fang, H. L.; Thrash, R. J.; Leroi, G. E. *J. Chem. Phys.* **1977**, *67*, 3389.

(16) Birge, R. R.; Bennett, J. A.; Pierce, B. M.; Thomas, T. M. *J. Am. Chem. Soc.* **1978**, *100*, 1533.

(17) Birge, R. R.; Bennett, J. A.; Fang, H. L.; Leroi, G. E. "Advances in Laser Chemistry". (Springer Series in Chemical Physics); Zewail, A. H., Ed.; Springer: New York, 1978; Vol. 3, pp 347–354.

(18) Birge, R. R.; Pierce, B. M. *J. Chem. Phys.* **1979**, *70*, 165.

0002-7863/82/1504-2519$01.25/0

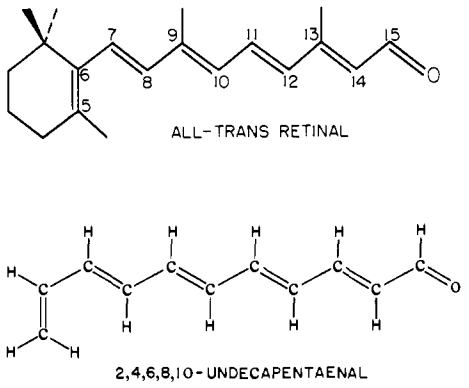

Figure 1. The structure and atom numbering convention of *all-trans*-retinal (top) and the structure of the polyene analogue (2,4,6,8,10-undecapentaenal, bottom) used to represent the chromophore portion of *all-trans*-retinal for the INDO–PSDCI calculations. In some calculations, the atomic coordinates of the undecapentaenal chromophore were determined using the cyrstal geometry of *all-trans*-retinal. These calculations are described under the heading "*all-trans*-retinal" to distinguish from those carried out on the planar, *all-trans* (*all-s-trans*) 2,4,6,8,10-undecapentaenal chromophore.

436 nm ($\lambda_{ex}/2$).[17] Although this wavelength range included the two-photon excitation maximum, it was not sufficient to provide information concerning the total excitation bandshape or the two-photon properties of the higher energy "$^1B_u{}^{*+}$" state. The two-photon excitation spectrum reported in this paper extends from 375–470 nm ($\lambda_{ex}/2$) and provides a measure of the relative two-photon absorptivities of the "$^1A_g{}^{*-}$" and "$^1B_u{}^{*+}$" states. Our previous analysis of *all-trans*-retinal[17] was based on the assumption that the two-photon excitation spectrum should be corrected for the wavelength dependence of the fluorescence quantum yield.[19] After ref 17 was in press, a paper by Takemura et al. was published which demonstrates that the wavelength dependence in the one-photon excitation spectrum is due to the presence of two retinal species, a "hydrogen-bonded" fluorescing species and a non-fluorescing species which acts as an "inner filter".[5] This "inner-filter effect" is not observable in two-photon excitation experiments where an insignificant fraction of the incident laser excitation is actually absorbed,[20] and therefore our previous wavelength dependent fluorescence quantum yield corrections should not have been applied. This correction resulted in a slight blue shift of the excitation maximum.[17] We previously reported a separation of 1950 ± 300 cm^{-1} between the "$^1B_u{}^{*+}$" one-photon and "$^1A_g{}^{*-}$" two-photon maxima;[17] our revised value for this separation is 2400 ± 300 cm^{-1} (see below).

One important question that has not been previously discussed in the literature is the extent to which the polarity and conformational distortion of *all-trans*-retinal "mixes" the low-lying "$^1B_u{}^{*+}$" and "$^1A_g{}^{*-}$" $\pi\pi^*$ states. Our experimental results provide new insights into this interaction and demonstrate that both the "$^1A_g{}^{*-}$" and "$^1B_u{}^{*+}$" states qualitatively retain the primary photophysical properties characteristic of their parent states in linear polyenes. The extent of "mixing" is at most 0.2 (where 1.0 represents complete mixing) based on our spectroscopic analysis of one-photon and two-photon intensity borrowing. Nonetheless, this mixing is sufficient to induce observable one-photon allowedness into the "$^1A_g{}^{*-}$" ← S_0 transition and two-photon allowedness into the "$^1B_u{}^{*+}$" ← S_0 transition.

II. Experimental Section

A schematic diagram of the two-photon excitation spectrometer is shown in Figure 2. The 337-nm output from a 900-kW nitrogen laser (Molectron UV24) is used to pump a tunable dye laser, amplifier combination (Molectron DL14). The two-photon excitation spectrum of *all-trans*-retinal was obtained with laser excitation from 750 to 940 nm. The dye laser generates a 7-ns pulse with better than 0.05 mJ pulse energy (0.1 mJ on average) throughout this wavelength range. The low-lying "$^1A_g{}^{*-}$" state of *all-trans*-retinal has a very high two-photon absorptivity ($\langle\delta\rangle_{calcd}^{max} \cong 3 \times 10^{-49}$ cm^4 s molecule^{-1} photon^{-1}; see below) and a reasonable quantum yield of fluorescence (~0.01). We found that pulse energies of ≥0.05 mJ are adequate to generate observable two-photon-induced fluorescence from *all-trans*-retinal (EPA 77 K) and further amplification using the external flash-lamp pumped amplifier shown in Figure 2 is not necessary.

The laser excitation was focused using an 85-mm achromatic lens into a cylindrical quartz cell containing *all-trans*-retinal (1.0×10^{-3} M) in degassed EPA (ethyl ether–isopentane–alcohol, 5:5:2 v/v) immersed in liquid nitrogen (77 K). The two-photon-induced fluorescence of *all-trans*-retinal was monitored perpendicular to the laser excitation beam through a Corning 4-65 glass filter in series with a 5-cm cell containing a saturated (~1.2 M) solution of $CuSO_4$. Although the transmission maximum of this filter combination ($\lambda_{max} \simeq 490$ nm) is to the blue of the emission maximum of *all-trans*-retinal ($\lambda_{max} \simeq 530$ nm), this filter combination is completely effective in blocking scattered laser light in the wavelength range 650–940 nm. The use of an RCA 1P28 photomultiplier to detect the fluorescence further improved discrimination of scattered laser light because this photomultiplier exhibits a very low quantum efficiency above 700 nm.

The pulse energy of the laser excitation was monitored using a pyroelectric joulemeter with a sensitivity of 9.89 V/mJ (Molectron Model J3). Standard boxcar signal averaging techniques were used to analyze both sample fluorescence and laser excitation energies using the sync pulse from the nitrogen laser to provide the trigger signal. A more detailed description of the two-photon excitation spectrometer may be found in ref 21.

The two-photon origin of the observed fluorescence signal was verified by determining the slope of log (I_f) vs. log (I_r) at selected wavelengths (750, 803, 840, and 883 nm) using neutral density filters to attenuate the laser excitation beam. The individual slopes calculated using least-squares techniques were equal to 2 ± S, where S is the standard error in the slope regression coefficient.

As noted in the Introduction, the two-photon excitation spectrum was not corrected for the apparent wavelength dependence of the fluorescence quantum yield. This wavelength dependence is due to competitive absorption by nonfluorescing species[5] and is not observable in two-photon excitation experiments where an insignificant fraction of the laser excitation is abosrbed.[20]

III. Theoretical

Wave functions for the ground and excited electronic states of *all-trans*-retinal were calculated using PPP-CISD[6,22,23] and INDO–PSDCI[7,24] molecular orbital procedures. The restricted π-electron PPP–CISD procedures included all possible (36) single and all possible (666) double excitations in the CI Hamiltonian. Repulsion integrals were calculated using the Ohno formula.[25] Resonance integrals were calculated using the Roos and Skancke relationship.[26] The following semiempirical parameters were adopted: $Z_c = 1.0$, $Z_{c'} = 1.1$, $Z_o = 0.9$, $I_c = -11.16$ eV, $I_{c'} = -12.29$ eV, $I_o = -16.02$ eV, $\langle\mu\mu|\mu\mu\rangle_c = 11.13$ eV, $\langle\mu\mu|\mu\mu\rangle_{c'} = 11.68$ eV, $\langle\mu\mu|\mu\mu\rangle_o = 14.49$ eV, $\beta_o = -2.43$, where c′ is the carbonyl carbon. A thorough discussion of the PPP–CISD formalism may be found in ref 27.

(19) Christensen, R. L.; Kohler, B. E. *Photochem. Photobiol.* **1974**, *19*, 401.

(20) The inner filter effect mechanism proposed by Takemura et al.[5] to explain the anomalous red shift of the one-photon fluorescence excitation spectrum relative to the one-photon absorption spectrum will not have any observable effect on the two-photon fluorescence excitation spectrum. The reason this effect is not observable in two-photon excitation spectroscopy is due to the negligible amount of laser light absorbed via two-photon excitation. The following calculation illustrates this prediction using data relevant to the present investigation: $\delta_{max} = 3 \times 10^{-49}$ cm^4 s molecule^{-1} photon^{-1}, $C = 1 \times 10^{-3}$ M $= 6 \times 10^{17}$ molecules cm^{-3}, $L = 1$ cm, $N = 1 \times 10^{15}$ photons/pulse, a Gaussian laser pulse width of 7 ns, and a focussed beam irradiated area of 0.001 cm^2. The number of photons absorbed via two-photon excitation will equal 1.704947×10^{10}. If we assume a second nonfluorescing species is present with the same two-photon absorptivity, a "worst case" inner-filtering of the laser pulse will lower the number of photons absorbed by the fluorescing species to 1.704889×10^{10}, a change of only 0.004%. This change is far too small to be experimentally observable.

(21) Bennett, J. A. Ph.D. Thesis, University of California, Riverside, Calif., 1980.

(22) Schulten, K.; Karplus, M. *Chem. Phys. Lett.* **1972**, *14*, 305.

(23) Tavan, P.; Schulten, K. *J. Chem. Phys.* **1979**, *70*, 5407.

(24) Hubbard, L. M. Ph.D. Thesis, University of California, Riverside, Calif., 1980.

(25) Ohno, K. *Theor. Chim. Acta* **1964**, *2*, 219.

(26) Roos, B.; Skancke, P. N. *Acta Chem. Scand.* **1967**, *21*, 233.

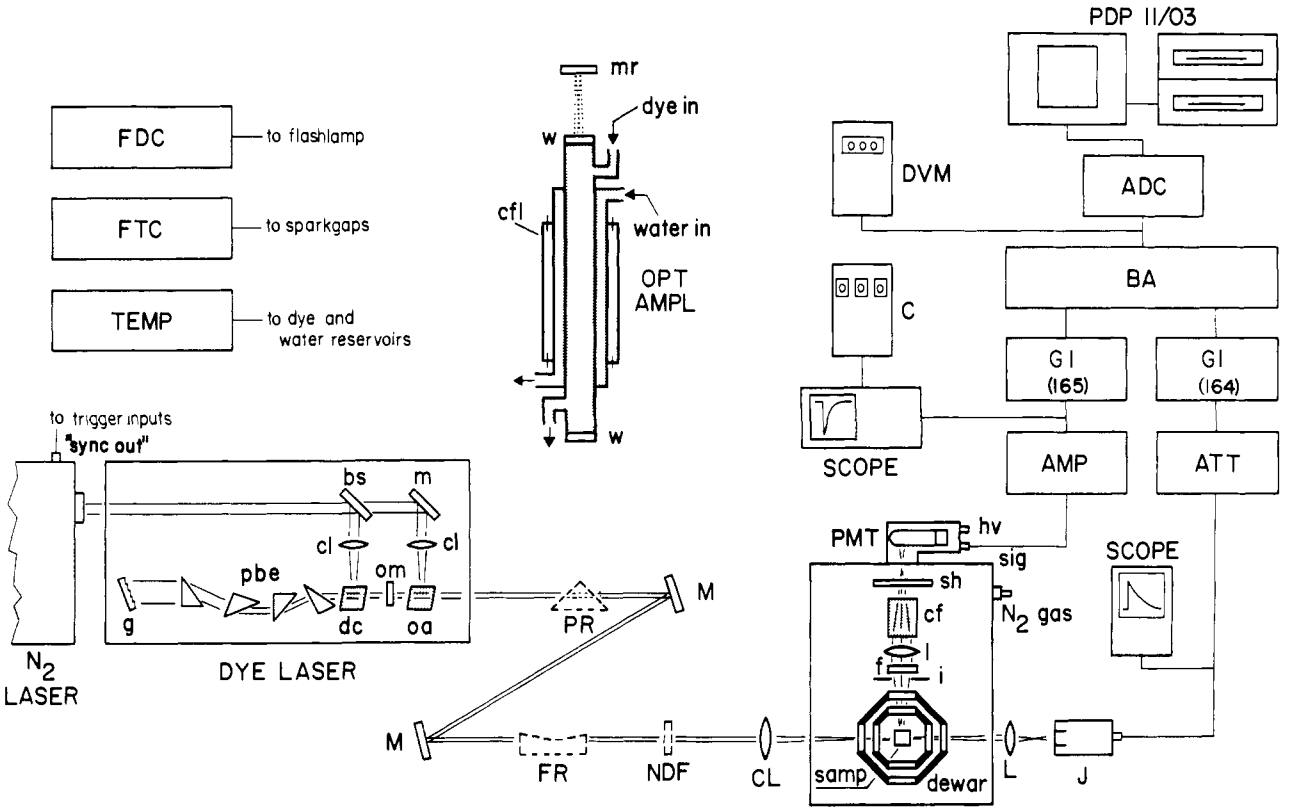

Figure 2. Nitrogen laser-pumped tunable dye laser two-photon excitation spectrometer. N_2 LASER = Molectron UV24 nitrogen laser (firing circuitry provides 200-ns "sync out" timing pulses for triggering boxcar averager); DYE LASER = Molectron DL14 UV–visible–near-IR tunable dye laser with optical amplifier (bs = beamsplitter, m = mirror, cl = condensing lens, g = diffraction grating, pbe = prism beam expander, dc = dye cuvette, om = output mirror, oa = optical amplifier dye cuvette); OPT AMPL = double-pass flashlamp-pumped optical amplifier (modified Phase-R DL 2100C "triax" dye laser; w = antireflection coated windows, cfl = coaxial flashlamp, mr = broad band maximum reflector); FDC = flashlamp driver circuit; FTC = flashlamp discharge timing circuit; TEMP = dye and water temperature controlling circuitry; PR = prism reflector; M = metal-surface mirror; FR = Fresnel rhomb, to convert linearly polarized laser light to circular or elliptical polarization; NDF = neutral density filters for attenuation of laser output; CL = achromatic condensing lens; dewar = optical dewar containing liquid nitrogen; samp = quartz or Pyrex cell containing sample; i = iris; f = glass filter; l = fluorescence-gathering lens; cf = chemical filter; sh = shutter to protect PMT from ambient light; PMT = RCA 1P28 photomultipiler tube; hv = connection to high-voltage power supply (not shown); sig = output signal from PMT due to sample fluorescence; N_2 gas = connector for dry nitrogen gas passed through dewar holder to keep dewar windows from fogging; L = lens to direct laser pulse (slightly defocused) onto pyroelectric detector element of joulemeter; J = joulemeter; AMP = short pulse amplifier; SCOPE = oscilloscope used to monitor output from amplifier or joulemeter and to adjust gate positions for gated integrators; C = electronic counter to count laser pulses; ATT = variable attenuation for joulemeter output; GI (164) = EG&G PAR Model 164 gated integrator to obtain average laser peak intensity; GI (165) = EG&G PAR Model 165 gated integrator, to obtain average sample peak fluorescence intensity; BA = EG&G PAR Model 162 boxcar averager mainframe (gated integrators are modules which plug into mainframe, shown separately for clarity); DVM = digital voltmeter to digitize analog outputs from each channel of boxcar averager; ADC = analog-to-digital converter (12-bit, 20 μs per conversion); PDP 11/03 = Terak Model 8510/8512 minicomputer with dual floppy disk storage.

The all-valence-electron INDO–PSDCI molecular orbital procedures were modeled after the CNDO/S procedures of Del Bene and Jaffe.[28] All single excitations below 13 eV (~120) and a selected number of the lowest energy double excitations determined using the ratio formula described in ref 7 (~300) were included. Repulsion integrals were calculated using the Mataga–Nishimoto formula.[29] Resonance integrals were calculated using the procedures of Del Bene and Jaffe which distinguishes between σ and π electron "mobility".[28] One-center repulsion and core parameters were taken from Sichel and Whitehead.[30] All of the INDO–PSDCI calculations were carried out using the "truncated" chromophore shown in the lower portion of Figure 1.

The error introduced in the calculation of the π-electron properties of the polyene chromophore as a result of the neglect of the C_9 and C_{13} methyl groups and the remaining portion of the β-ionylidene ring does not appear to be serious. For example, the ground-state dipole moment of *all-trans*-retinal (crystal geometry) is calculated to be 4.54 D using INDO–PSDCI This value is in reasonable agreement with two recent experimental measurements: 4.59 ± 0.07 D (Corsetti and Kohler, based on dielectric measurements and a spherical cavity approximation[31]) and 5.26 ± 0.16 D (Myers and Birge, based on dielectric measurements[32a] and an elliptical cavity approximation[32b]).

A problem inherent in both the PPP–CISD and INDO–PSDCI formalisms is due to the neglect of higher excitations (triple, quadruple, etc.) in the CI Hamiltonian. Tavan and Schulten[23] have discussed this problem as applied to the PPP formalism and have shown that neglect of higher levels of CI generates a size inconsistency and an imbalance in the degree to which various electronic states are stabilized by single and double excitation CI. Whereas single and double CI appears to adequately describe the relative level ordering of covalent and ionic $\pi\pi^*$ electronic states in hexaenes, the ground state is "overcorrelated" which generates unrealistically large transition energies.[6,16,18,23,27] The usual procedure is to calculate transition energies relative to the "uncorrelated" (SCF) ground state.[6] However, this approach does not work well for all situations because in some molecules there exist low-lying excited states which are spatially localized with

(27) Schulten, K. Ph.D. Thesis, Harvard University, Cambridge, Mass., 1975.
(28) Del Bene, J.; Jaffe, H. H. *J. Chem. Phys.* **1968**, *48*, 1807, 4050; **1968**, *49*, 1221.
(29) Mataga, N.; Nishimoto, K. *Z. Phys. Chem. (Frankfurt am Main)* **1957**, *13*, 140.
(30) Sichel, J. M.; Whitehead, M. A. *Theor. Chim. Acta* **1967**, *7*, 32.
(31) Corsetti, J. D.; Kohler, B. E. *J. Chem. Phys.* **1977**, *67*, 5237.
(32) (a) Myers, A. B.; Birge, R. R. *J. Am. Chem. Soc.* **1981**, *103*, 1881. (b) Myers, A. B.; Birge, R. R. *J. Chem. Phys.* **1981**, *74*, 3514.

respect to electron distribution relative to other more delocalized ($\pi\pi^*$) states. In this case the problem of "size consistency" becomes important even for a single molecular system, and localized $\pi\pi^*$ or $\sigma\pi^*$ excited states are predicted to have unrealistically low transition energies when the uncorrelated SCF ground state is used. Bennett and Birge have discussed this problem with reference to PPP–CISD calculations on diphenylbutadiene in which a $^1A_g{}^{*-}$ $\pi\pi^*$ state localized in the phenyl groups is falsely predicted to be lower in energy than a $^1A_g{}^{*-}$ $\pi\pi^*$ state delocalized throughout the π-electron system.[12] A similar problem arises in the application of INDO–PSDCI theory to polyenals. The relatively localized $\pi^* \leftarrow$ n transition is predicted to be lower in energy than is experimentally observed when the excitation energy is calculated relative to the uncorrelated ground state. A much better fit to experimental data is achieved when the excitation energy of the $\pi^* \leftarrow$ n transition is calculated relative to the correlated ground state.[24] Accordingly, we have calculated $\pi^* \leftarrow \pi$ transition energies using the uncorrelated ground state and $\pi^* \leftarrow$ n transition energies using the correlated ground state. Given the artificial nature of this approach we do not expect our INDO–PSDCI procedures to be accurate for calculations of the level ordering of the $n\pi^*$ states relative to nearby $\pi\pi^*$ states. However, the general one-photon and two-photon properties of the low-lying $n\pi^*$ and $\pi\pi^*$ states (e.g., calculated oscillator strengths and two-photon absorptivities) are not overly sensitive to small changes in transition energy, and we have greater confidence in the accuracy of these calculated values.

The two-photon properties of the excited states are calculated using the procedures described by Birge and Pierce.[18] The basis set of intermediate states contained the ten lowest electronic states (N = 10 in eq 1, 2, 4–7 of ref 18). Although the initial and final states should normally be included in the summation over intermediate states (see ref 33), they were not included in the calculations reported here. We neglected these contributions because they are proportional to the changes in the dipole moment upon excitation. Neither the PPP–CISD nor the INDO–PSDCI calculations included the entire retinyl framework. The PPP–CISD calculations significantly underestimate the dipole moments whereas the INDO–PSDCI calculations appear to underestimate the ground-state dipole moment and overestimate the excited-state dipole moments of the $\pi\pi^*$ states. We conclude that the accuracy of our calculations would be decreased by the inclusion of the initial and final states in the summation over intermediate states.

IV. Results and Discussion

The two-photon excitation spectrum of *all-trans*-retinal in EPA (77 K) is shown in Figure 3. The spectrum was obtained using linearly polarized laser excitation and is plotted as a function of (laser wavelength)/2 to facilitate comparison with the one-photon absorption spectrum. The dashed line representing the two-photon excitation curve was generated using a three-point triangular smoothing function followed by five-point Lagrangian interpolation.

(A) Analysis of One-Photon and Two-Photon Spectra. Both the one-photon absorption spectrum and the two-photon excitation spectrum are broad and unstructed and exhibit severe inhomogeneous broadening.[34] This observation precludes the assignment of system origins of the electronic states responsible for the one-photon and two-photon spectra. Our analysis indicates that the "$^1B_u{}^{*+}$" state contributes >90% of the oscillator strength of the one-photon absorption band whereas the "$^1A_g{}^{*-}$" state contributes >83% of the absorptivity to the two-photon excitation band (see below). Accordingly, the λ_{max} separation of 2400 ± 300 cm^{-1} observed in the spectra shown in Figure 3 represents to good approximation the separation of the vibronic maxima of the "$^1B_u{}^{*+}$" and "$^1A_g{}^{*-}$" states. Accordingly, the "$^1A_g{}^{*-}$" state is approximately 2400 cm^{-1} lower in energy than the "$^1B_u{}^{*+}$" state in *all-trans*-retinal in EPA (77 K).

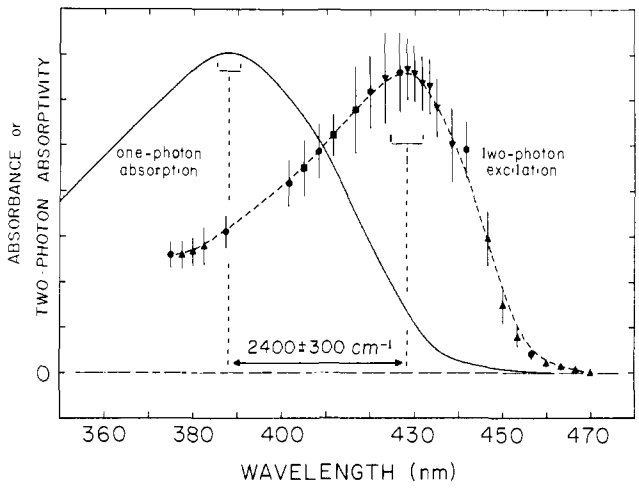

Figure 3. Comparison of the two-photon excitation spectrum (dashed line) and the one-photon absorption spectrum (solid line) of *all-trans*-retinal in EPA solvent at 77 K. The two-photon data are plotted as a function of (laser excitation wavelength/2). The solid circles represent a single experiment carried out by measuring the two-photon excitation signal (I_f/I_r^2) at discrete wavelengths corresponding to the lasing maxima of the following dyes: oxazine 725 perchlorate (750 nm); DOTC (775 nm); DOTC:HITC, 3:2 (803.2 nm); DOTC:HITC, 1:1 (816.8 nm); HITC (840 nm); DTTC (852 nm); IR 144 (883.2); IR 125 (913.2 nm). This experiment was carried out without touching the sample or adjusting any of the optics. The remaining symbols represent data obtained using some of the above dyes to "fill in" between the above measurements and were scaled to be coincident at the "edges" with the solid circle measurements. This approach is necessary because it is impossible to place the sample cell in the dewar at precisely the same location for each data collection run. The scaling in each case, however, was small (<10%). All of the symbols represent an average of at least 150 laser shots, and the height of the vertical lines are equal to twice the sample standard deviation plus the predicted scaling error.

The molecular orbital calculations described below predict that "$^1A_g{}^{*-}$" and "$^1B_u{}^{*+}$" states are mixed to generate one-photon allowedness in the "$^1A_g{}^{*-}$" $\leftarrow S_0$ transition and two-photon allowedness in the "$^1B_u{}^{*+}$" $\leftarrow S_0$ transition (see section IV B). We addressed this question from an experimental standpoint by fitting the one-photon and two-photon spectra to two long-normal curves.[35] The details are described in the suppplementary material that appears at the end of this paper in the microfilm edition and the results are summarized in Table I. The relatively large error bars for the assigned values listed in Table I reflect the lack of precision inherent in this approach. Nonetheless, these data provide a useful qualitative picture of the extent to which the low-lying covalent and ionic $\pi\pi^*$ states are mixed in *all-trans*-retinal. We discuss our experimental results in more detail below where a comparison is made with the predictions of our molecular orbital calculations.

(B) Molecular Orbital Calculations. A comparison of the calculated and observed one-photon and two-photon properties of the "$^1A_g{}^{*-}$" and "$^1B_u{}^{*+}$" $\pi\pi^*$ excited states of *all-trans*-retinal is presented in Table I. A comparison of the theoretical predictions of the PPP–CISD and INDO–PSDCI formalisms is also shown in Figure 4. Before we analyze the comparative accuracy of these two formalisms, we will consider the importance of the $n\pi^*$ state in terms of its possible contribution to the one-photon and two-photon spectra. The question is relevant because our analysis of the experimental spectra totally neglects any contribution of the $n\pi^*$ state to the band profiles; we demonstrate below that this neglect is justified.

(1) One-Photon and Two-Photon Properties of the $\pi^* \leftarrow$ n Transition. The INDO–PSDCI calculations predict a low-lying $n\pi^*$ state which is nearly degenerate with the lowest lying "$^1A_g{}^{*-}$" $\pi\pi^*$ state. As noted in the theoretical section, however, we cannot rely on the INDO–PSDCI formalism to accurately predict the

(33) Mortensen, O. S.; Svendsen, E. N. *J. Chem. Phys.* **1981**, *74*, 3185.
(34) Christensen, R. L.; Kohler, B. E. *Photochem. Photobiol.* **1973**, *18*, 293.
(35) Metzler, D. E.; Harris, C. M. *Vision Res.* **1978**, *18*, 1417.

Table I. Comparison of Observed and Calculated One-Photon and Two-Photon Properties of the "$^1A_g{}^{*-}$" and "$^1B_u{}^{*+}$" $\pi\pi^*$ Excited States of *all-trans*-Retinal

property (units)	PPP-CISD[a]	INDO-PSDCI[b]	observed[c]
$\Delta E[\text{"}^1B_u{}^{*+}\text{"} \leftarrow S_0]$[d] (eV)	3.411	3.531	3.20 ± 0.01
$f[\text{"}^1B_u{}^{*+}\text{"} \leftarrow S_0]$[e]	0.965	1.099	1.18 ± 0.05
$\Delta E[\text{"}^1A_g{}^{*-}\text{"} \leftarrow S_0]$[d] (eV)	3.172	3.256	2.90 ± 0.02
$f[\text{"}^1A_g{}^{*-}\text{"} \leftarrow S_0]$[e]	0.251	0.125	0.07 ± 0.05
$\Delta\Delta E[\text{"}^1B_u{}^{*+}\text{"} - \text{"}^1A_g{}^{*-}\text{"}]$[f] ($cm^{-1}$)	1928	2218	2400 ± 300
$f[\lambda_{max}]$[g]	1.216	1.224	1.24 ± 0.02
$\delta_{max}(\text{"}^1B_u{}^{*+}\text{"} \leftarrow S_0)$[h] (marias)	14.17	13.80	
$\Omega(\text{"}^1B_u{}^{*+}\text{"} \leftarrow S_0)$[i]	0.679	0.686	
$\delta_{max}(\text{"}^1A_g{}^{*-}\text{"} \leftarrow S_0)$[h] (marias)	29.93	69.92	
$\Omega(\text{"}^1A_g{}^{*-}\text{"} \leftarrow S_0)$[i]	0.693	0.668	
$\delta_{max}(\text{"}^1A_g{}^{*-}\text{"})/\delta_{max}(\text{"}^1B_u{}^{*+}\text{"})$[j]	2.112	5.067	6.9 ± 1.0

[a] Calculated values based on PPP-CISD procedures including full single and double excitation CI (see text). Atomic coordinates were determined using the crystal geometry of *all-trans*-retinal (ref 36). [b] Calculated values based on INDO-PSDCI procedures including partial single and partial double excitation CI (see text). Atomic coordinates were determined using the crystal geometry of *all-trans*-retinal (ref 36). [c] All values for *all-trans*-retinal in EPA (77 K). [d] Transition energy at maximum absorption or maximum absorptivity. [e] One-photon oscillator strength. [f] Energy difference between the "$^1B_u{}^{*+}$" and the "$^1A_g{}^{*-}$" state maxima. [g] Total oscillator strength of the one-photon λ_{max} absorption band including contributions from both the "$^1B_u{}^{*+}$" $\leftarrow S_0$ and "$^1A_g{}^{*-}$" $\leftarrow S_0$ transitions. [h] Two-photon absorptivity at maximum in marias (1.0×10^{-50} cm^4 s molecule^{-1} photon^{-1}) for two linearly polarized photons of equal polarization and energy. [i] Two-photon polarization ratio (see ref 18). [j] Two-photon absorptivity at maximum for the "$^1A_g{}^{*-}$" $\leftarrow S_0$ transition divided by that for the "$^1B_u{}^{*+}$" $\leftarrow S_0$ transition.

level ordering of the $n\pi^*$ state in relation to nearby $\pi\pi^*$ states. The observation that *all-trans*-retinal fluoresces at 77 K in EPA suggests, however, that a lowest lying $\pi\pi^*$ state exists for many of the *all-trans*-retinal species in low-temperature polar solvent glasses. Accordingly, the level ordering depicted in Figure 4 is not unrealistic. The salient conclusion of the INDO–PSDCI calculations is that the $\pi^* \leftarrow n$ transition has negligible one-photon and two-photon absorptivities,

The one-photon $\pi^* \leftarrow n$ transition in short-chain substituted and unsubstituted polyenals is very weak ($f \sim 4 \times 10^{-4}$, ref 37). INDO–PSDCI theory predicts oscillator strengths for the short-chain polyenals in excellent agreement with experiment,[24] and this observation suggests that the calculations on the $\pi^* \leftarrow n$ transition of *all-trans*-retinal should be realistic, Furthermore, mixing of allowed excited states into the $n\pi^*$ state due to conformational distortion of the retinal skeleton[38] should be properly accounted for in our INDO–PSDCi calculations because we used the crystal geometry[36] to assign the atomic coordinates of our model chromophore. In summary, we believe our calculations adequately describe the one-photon oscillator strength of the $\pi^* \leftarrow n$ transition.

The INDO–PSDCI calculations indicate that the $\pi^* \leftarrow n$ transition in *all-trans*-retinal is weak primarily because of poor atomic orbital overlap associated with the n and π^* molecular orbitals. A significant fraction of the oscillator strength derives from one-center $\langle\phi_{2s}|er|\phi_{2p_z}\rangle$ contributions which are inherently small.[39] The $\pi^* \leftarrow n$ transition is therefore polarized primarily

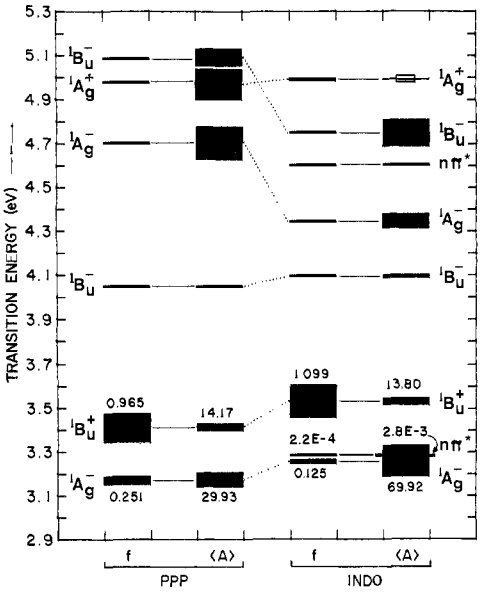

Figure 4. Calculated one-photon oscillator strengths (f) and maximum two-photon absorptivities $\langle A\rangle$ for the low-lying excited singlet states of *all-trans*-retinal based on PPP–CISD and INDO–PSDCI procedures. The electronic states are represented with horizontal bars, where the vertical position indicates the transition energy and the vertical width is proportional to f or $\langle A\rangle$. The two-photon absorptivities are in units of 10^{-50} cm^4 s molecule^{-1} photon^{-1} and are calculated for two linearly polarized photons of equal energy, polarization, and propagation. The symmetry labels are approximate. The two-photon absorptivity of the "$^1A_g{}^{*+}$" state calculated using INDO–PSDCI theory is strongly enhanced by resonance and is indicated using an open rectangle.

out of the plane of the retinyl chromophore. These observations help to explain why the $\pi^* \leftarrow n$ transition is calculated to exhibit a very small two-photon absorptivity (Figure 4). A single intermediate state approximation for the two-photon absorptivity yields:[18]

$$\langle\delta\rangle_{max}^{n\pi^*} = \left[\frac{(2\pi e)^4}{30c^2h^2}\right] E_\lambda{}^2 g_{max}(S_{ab}^{n\pi^*} + S_b^{n\pi^*}) \qquad (1a)$$

where

$$S_{ab}^{n\pi^*} = (a + b)[\langle\pi\pi^*|r|S_0\rangle\cdot\langle n\pi^*|r|\pi\pi^*\rangle]^2(E_{\pi\pi^*} - E_\lambda)^{-2} \qquad (1b)$$

and

$$S_b^{n\pi^*} = b|\langle\pi\pi^*|r|S_0\rangle|^2|\langle n\pi^*|r|\pi\pi^*\rangle|^2(E_{\pi\pi^*} - E_\lambda)^{-2} \qquad (1c)$$

E_λ is the energy of the laser excitation, g_{max} is the maximum value of the normalized line-shape function, $E_{\pi\pi^*}$ is the energy of the strongly one-photon allowed intermediate state (assumed to be a low-lying $\pi\pi^*$ state), and a and b are the photon polarization–propagation variables (Table I of ref 18). The low-lying "$^1B_u{}^{*+}$" $\pi\pi^*$ state is the dominant intermediate state for two-photon excitation processes in *all-trans*-retinal. The "$^1B_u{}^{*+}$" $\leftarrow S_0$ transition is polarized in the plane of the molecule whereas the $\pi^* \leftarrow n$ transition is primarily polarized perpendicular to the molecular plane (see above). Accordingly, the dot product of the transition length vectors in eq 1b approaches zero, and $S_{ab} \sim 0$. The transition energies of the $n\pi^*$ and "$^1B_u{}^{*+}$" states are both ~3.3 eV (Figure 4) and therefore $E_\lambda \sim {}^1/_2\, E_{\pi\pi^*}$. Equation 1 reduces to

$$\langle\delta\rangle_{max}^{n\pi^*} = (7.0 \times 10^{-5})b(g_{max})|\langle\pi\pi^*|r|S_0\rangle|^2|\langle n\pi^*|r|\pi\pi^*\rangle|^2 \qquad (2)$$

The reason the $\pi^* \leftarrow n$ transition of *all-trans*-retinal has a negligible two-photon absorptivity is that the magnitude of the transition length vector, $\langle n\pi^*|r|\pi\pi^*\rangle$, is extremely small ($\sim 10^{-4}$ Å). This term is small for reasons identical with those mentioned above to explain the small one-photon oscillator strength of the $\pi^* \leftarrow n$ transition, namely, poor atomic orbital overlap. We can make the following generalization: *if the* $\pi^* \leftarrow n$ *transition*

(36) Hamanaka, T.; Mitsui, T.; Ashida, T.; Kakudo, M. *Acta Crystallogr., Sect. B* **1972**, *28*, 214.
(37) Birge, R. R.; Leermakers, P. A. *J. Am. Chem. Soc.* **1972**, *94*, 8105, and references therein.
(38) Weimann, L. J.; Maggiora, G. M.; Blatz, P. *Int. J. Quantum Chem.* **1975**, *2*, 9.
(39) Ellis, R. L.; Kuehnlenz, G.; Jaffe, H. H. *Theor. Chim. Acta* **1972**, *26*, 131.

Table II. Comparison of PPP-SCF and INDO-SCF Calculations for *all-trans*-2,4,6,8,10-Undecapentaenal

	PPP-SCF[a]				INDO-SCF[b]			
atom[c]	π(HOMO)[d]	π^*(LUMO)[e]	$P_{\pi\pi}$(SCF)[f]	q_{atom}[g]	π(HOMO)[d]	π^*(LUMO)[e]	$P_{\pi\pi}$(SCF)[f]	q_{atom}[h]
C_5	0.3330	0.2301	0.9883	0.0117	0.3315	0.2584	1.0109	−0.0536
C_6	0.1836	−0.0970	1.0053	−0.0053	0.1608	−0.1117	0.9877	−0.0038
C_7	−0.3876	−0.3125	0.9832	0.0168	−0.3834	−0.3299	0.9926	−0.0086
C_8	−0.3265	0.1934	1.0106	−0.0106	−0.2991	0.2125	1.0012	−0.0163
C_9	0.3519	0.3670	0.9737	0.0263	0.3580	0.3650	0.9844	−0.0074
C_{10}	0.3943	−0.2785	1.0177	−0.0177	0.3779	−0.2947	1.0073	−0.0193
C_{11}	−0.2473	−0.3787	0.9573	0.0427	−0.2648	−0.3561	0.9707	0.0007
C_{12}	−0.3766	0.3391	1.0289	−0.0289	−0.3822	0.3462	1.0150	−0.0215
C_{13}	0.1122	0.3303	0.9260	0.0740	0.1286	0.2978	0.9332	0.0212
C_{14}	0.2897	−0.3627	1.0540	−0.0540	0.3161	−0.3524	1.0348	−0.0306
C_{15}	0.0198	−0.2123	0.6517	0.3483	0.0216	−0.1907	0.7695	0.2753
O	−0.1390	0.2148	1.4031	−0.4031	−0.1537	0.2256	1.2928	−0.3691
H's								0.2330

parameter	PPP-SCF	PPP-CISD	INDO-SCF	INDO-PSDCI
$\mu(S_0)$[i]	4.397 D	3.742 D[k]	3.779 D	3.420 D[l]
$\mu(S_0)_{tot}$[j]	na	na	4.606 D	4.373 D[l]

[a] PPP-SCF calculation using a standard geometry which is planar all-trans (all-s-trans) with all angles 120° and standard bond lengths ($R_{C=C}$ = 1.35 Å, R_{C-C} = 1.46 Å, $R_{C=O}$ = 1.22 Å). [b] INDO-SCF calculation using standard geometry described in (a) and carbon-hydrogen bond lengths of 1.08 Å except $R_{C-H_{ald}}$ = 1.11 Å. [c] Atoms are numbered using retinal convention. The hydrogen atom's net charge only applies to INDO calculations. [d] Eigenvectors for the highest energy occupied π molecular orbital. [e] Eigenvectors for the lowest energy unoccupied π^* molecular orbital. [f] Charge density in the SCF ground state π electron manifold. [g] Atomic charges in the SCF ground state. [h] Atomic charges in the SCF ground state. Values include σ system contributions. All of the hydrogen atoms are positively charged and only the total charge on all 12 hydrogens is listed. [i] Ground-state dipole moment calculated from atomic charges. [j] Ground-state dipole moment including contribution from one-center *sp* hybridization (INDO only); (na = not applicable). [k] Ground-state dipole moment from CI calculation including 36 single and 666 double excitations. [l] Ground-state dipole moment from CI calculation including 114 single and 219 double excitations.

Table III. Conformational and Configurational Characteristics of the Low-Lying Excited States in *all-trans*-Retinal and *all-trans*-2,4,6,8,10-Undecapentaenal

	undecapentaenal[a]			*all-trans*-retinal[b]		
calcd property or character	$n\pi^*$	"$^1A_g{}^{*-}$"	"$^1B_u{}^{*+}$"	$n\pi^*$	"$^1A_g{}^{*-}$"	"$^1B_u{}^{*+}$"
ΔE (eV)[c]	3.2509	3.1923	3.5212	3.2753	3.2555	3.5314
dipole moment (D)[d]	0.9334	7.8533	8.1949	1.5994	9.0828	7.9918
DCI character (%)[e]	11.1	54.8	7.9	14.7	43.6	13.2
σ character (%)[f]	55	0	0	52	6	3

[a] All-trans (all-s-trans) geometry as described in footnote *b* of Table II. [b] Crystal geometry (ref 36). [c] Transition energy. [d] Dipole moment of excited state in debyes. Ground-state dipole moments are 4.373 D (undecapentaenal) and 4.543 (*all-trans*-retinal). [e] Percent doubly excited character. [f] Percent of σ electron character.

exhibits a negligible one-photon oscillator strength, it will exhibit a negligible two-photon absorptivity. In summary, therefore, our assumption that the $\pi^* \leftarrow$ n transition can be ignored in the analysis of the one-photon and two-photon spectra shown in Figure 3 is justified.

(2) One-Photon and Two-Photon Properties of the "$^1A_g{}^{*-}$" and "$^1B_u{}^{*+}$" States. Analysis of Table I indicates that both the PPP–CISD and INDO–PSDCI procedures overestimate the one-photon oscillator strength of the "$^1A_g{}^{*-}$" $\leftarrow S_0$ transition and the two-photon absorptivity of the "$^1B_u{}^{*+}$" state relative to the "$^1A_g{}^{*-}$" state. In other words, both formalisms overestimate the amount of "$^1A_g{}^{*-}$" – "$^1B_u{}^{*+}$" excited-state "mixing". The INDO–PSDCI procedures, however, appear to be more accurate than the PPP–CISD procedures. We attribute this observation to the importance of σ-electron polarization effects which serve to decrease the calculated degree of π-electron polarization. As shown in Table II, the ground-state π-electron system of the planar *all-trans*-undecapentaenal is predicted by PPP–SCF theory to be much more polarized by the carbonyl group than is predicted by INDO–SCF theory. (We have chosen to use *all-trans*-undecapentaenal as a test chromophore because the σ and π electron manifolds are separable into different atomic orbitals of the all-valence-electron INDO basis set. This facilitates the comparison of the PPP and INDO wave functions.) Although it might appear possible to improve the PPP–CISD calculations by modifying the semiempirical parameters so that the PPP–SCF π-electron wave functions more closely mimic the INDO–SCF wave functions, this approach is unlikely to be globally successful. The problem is one inherent to any restricted π-electron basis set procedure, and a set of semiempirical parameters that works well for one conformation may fail when applied to a different conformation. The σ-electron system must be included if one is to properly describe the π-electron system in a polar molecule like retinal.

(3) Conformational Properties of the Low-Lying Excited States. The discussion presented in the previous sections indicates that the INDO–PSDCI procedures are more accurate than the PPP–CISD procedures in predicting the photophysical properties of the low-lying $\pi\pi^*$ states of *all-trans*-retinal. The following analysis is based entirely on INDO–PSDCI calculations.

Table III presents a comparison of the calculated properties of the low-lying singlet states as a function of geometry. Analysis of this table indicates that conformational distortion of the retinal chromophore results in a loss of doubly excited character in the "$^1A_g{}^{*-}$" state (−11%) and a gain of doubly excited character in the $n\pi^*$ (+3.6%) and "$^1B_u{}^{*+}$" (+5.3%) states. The "$^1A_g{}^{*-}$" and "$^1B_u{}^{*+}$" states gain a small amount of σ-electron character as a result of conformational distortion. The conformational distortion induces a significant amount of state mixing which serves to increase the one-photon allowedness of the "$^1A_g{}^{*-}$" state and the two-photon allowedness of the "$^1B_u{}^{*+}$" state. An analysis of Tables I–III indicates that both polarity and conformational distortion are of approximately equal importance in generating excited-state mixing. Analogous INDO–PSDCI calculations on distorted decapentaenes ($C_{10}H_{12}$) indicate that comparable conformational distortion of a nonpolar chromophore does not induce significant state mixing.[24] Accordingly, polarity is a necessary requirement to induce observable excited-state mixing, but conformational

distortion of a polar polyene enhances the extent of mixing.

(C) Solvent Effects. Our experiments were carried out in a polar solvent glass (EPA) at 77 K. It is useful to qualitatively speculate on the effect that solvent polarity and refractive index have on the observed photophysical properties of the $n\pi^*$, "$^1B_u{}^{*+}$", and "$^1A_g{}^{*-}$" excited states. In particular, we demonstrate that the "$^1A_g{}^{*-}$" state is likely to be the lowest lying $\pi\pi^*$ state in the vast majority of solvent environments and temperatures. The relative level ordering of the $n\pi^*$ state, however, is likely to be strongly influenced by solvent environment as proposed by Takemura et al.[5]

Corsetti and Kohler have studied the effect of solvent polarity and polarizability on the absorption spectrum of *all-trans*-retinal.[31] These authors observed a red shift in the absorption maximum as a function of increased solvent polarity or as a function of increased solvent polarizability. These results indicate that the "$^1B_u{}^{*+}$" state, the major contributor to the λ_{max} band (Table I), has a larger dipole moment ($\mu_e \sim 6$ D) and a higher polarizability ($\alpha_e \sim 130$ Å^3) than the ground state ($\mu_g \sim 4.6$ D, $\alpha_g \sim 110$ Å^3).[31] The INDO–PSDCI calculations are in reasonable agreement with the dipole moment measurements, although our calculated excited-state dipole moment for the "$^1B_u{}^{*+}$" state ($\mu_e^{calcd} \sim 8$ D, Table III) appears to be overestimated. However, Corsetti and Kohler used a spherical cavity reaction field which will tend to underestimate the dipole moments of molecules, like *all-trans*-retinal, which are "elongated" in the direction of the dipole moment.[32]

The INDO–PSDCI calculations indicate that the "$^1A_g{}^{*-}$" and "$^1B_u{}^{*+}$" states have very similar dipole moments (Table III). Accordingly, solvent polarity changes are unlikely to produce a level inversion of these two states. The $n\pi^*$ state, however, is calculated to have a significantly lower dipole moment than the ground state (Table III), and therefore increasing solvent polarity will blue shift this state. Our calculations are therefore in essential agreement with the arguments presented by Takemura et al.[5]

The observation that the "$^1A_g{}^{*-}$" state has a lower oscillator strength than the "$^1B_u{}^{*+}$" state (Table I) suggests that increasing solvent polarizability will preferentially red shift the "$^1B_1{}^{*+}$" state relative to the "$^1A_g{}^{*-}$" state. This effect will bring the two electronic states into closer energetic proximity and presumably enhance their interaction. An approximate analysis based on the approach of Sklar et al.[40] yields

$$\Delta\tilde{\nu} = \Delta\tilde{\nu}_0 - \Delta K[(n^2 - 1)/(n^2 + 2)] \quad (3)$$

where $\Delta\tilde{\nu}$ is the "$^1B_u{}^{*+}$"–"$^1A_g{}^{*-}$" wavenumber separation, $\Delta\tilde{\nu}_0$ is the above separation for the free chromophore, ΔK is the difference in the dispersion constants,

$$\Delta K = K(\text{"}^1B_u{}^{*+}\text{"}) - K(\text{"}^1A_g{}^{*-}\text{"}) \quad (4)$$

and n is the refractive index of the solvent. Corsetti and Kohler have measured K("$^1B_u{}^{*+}$") for *all-trans*-retinal to be 9500 ± 1500 cm^{-1}.[31] Since K is proportional to the one-photon oscillator strength, $K(\text{"}^1A_g{}^{*-}\text{"}) \cong f(\text{"}^1A_g{}^{*-}\text{"}) \cdot K(\text{"}^1B_u{}^{*+}\text{"})/f(\text{"}^1B_u{}^{*+}\text{"}) \sim 1000 \pm 1500$ cm^{-1}, $\Delta K \sim 8500 \pm 2000$ cm^{-1}. The refractive index of EPA (77 K) is 1.469.[12] Thus, eq 3 predicts a free chromophore "$^1B_u{}^{*+}$"–"$^1A_g{}^{*-}$" wavenumber difference of

$$\Delta\tilde{\nu}_0 = \Delta\tilde{\nu} + \Delta K[(n^2 - 1)/(n^2 + 2)] = (2400 \pm 300 \text{ cm}^{-1}) + (8500 \pm 2000 \text{ cm}^{-1})(0.279) = 4800 \pm 900 \text{ cm}^{-1}$$

This calculation must be considered very approximate because we have neglected electrostatic solvent–solute interactions. However, the INDO–PSDCI calculations predict very similar excited-state dipole moments for the "$^1A_g{}^{*-}$" and "$^1B_u{}^{*+}$" states, which should result in comparable electrostatic red shifts upon increasing solvent polarity. Accordingly, the above analysis is probably reliable within the error range defined.

A solvent refractive index of at least 1.7, and probably a value significantly larger, would be necessary to invert the "$^1B_u{}^{*+}$" and "$^1A_g{}^{*-}$" $\pi\pi^*$ state level ordering. One may be confident that the vast majority of solution environments will preserve the level ordering (though not the energy separation) observed in this study.

V. Summary

(1) The "$^1A_g{}^{*-}$" $\pi\pi^*$ excited state is the lowest lying $\pi\pi^*$ state in *all-trans*-retinal. The observed energy separation between the "$^1B_u{}^{*+}$" and the "$^1A_g{}^{*-}$" maxima is 2400 ± 300 cm^{-1} in EPA at 77 K. An approximate solvent-effect analysis predicts a free chromophore splitting of 4800 ± 900 cm^{-1}.

(2) The "$^1A_g{}^{*-}$" and "$^1B_u{}^{*+}$" states are "mixed" by a combination of conformational distortion and polarity effects in *all-trans*-retinal which combine in approximately equal proportion to induce one-photon allowedness into the "$^1A_g{}^{*-}$" ← S_0 transition and two-photon allowedness into the "$^1B_u{}^{*+}$" ← S_0 transition. Nevertheless, the one-photon oscillator strength of the "$^1B_u{}^{*+}$" ← S_0 transition is at least nine times larger than that observed for the "$^1A_g{}^{*-}$" ← S_0 transition. Similarly, the two-photon absorptivity of the "$^1A_g{}^{*-}$" ← S_0 transition is at least five times larger than that observed for the "$^1B_u{}^{*+}$" ← S_0 transition.

(3) The π^* ← n transition is extremely weak in both one-photon and two-photon spectroscopy because of poor atomic orbital overlap between the n and π^* molecular orbitals. We conclude that this transition is of no importance in affecting the band profiles of the one-photon absorption and the two-photon excitation spectra. The fact that *all-trans*-retinal fluoresces in EPA (77 K) indicates that many of the retinal species have a lowest lying "$^1A_g{}^{*-}$" $\pi\pi^*$ state in low-temperature polar glasses.

Acknowledgment. This work was supported in part by grants from the National Institutes of Health [EY-02202 (R.R.B)], the National Science Foundation [CHE-7916336 (R.R.B) and CHE-7921319 (G.E.L)], and the Committee on Research, University of California—Riverside. R.R.B. thanks Professors David Bocian, Tom Ebrey, Barry Honig, Bryan Kohler, and Klaus Schulten for interesting and helpful discussions. The authors thank Dr. Gordon Hug for pointing out that the inner filter effect is not important in two-photon excitation spectroscopy and for sending us his detailed derivation in support of this prediction.

Registry No. *all-trans*-Retinal, 116-31-4; *all-trans*-2,4,6,8,10-undecapentaenal, 41855-42-9.

Supplementary Material Available: The analysis of the one-photon absorption and two-photon excitation spectra of *all-trans*-retinal using log-normal distribution functions to describe the band profiles of the "$^1A_g{}^{*-}$" and "$^1B_u{}^{*+}$" states is described; the results of the analysis are given in Table I (see above) (4 pages). Ordering information is given on any current masthead page.

(40) Sklar, L.; Hudson, B.; Petersen, M.; Diamond, J. *Biochemistry* **1977**, *16*, 813.